PROCEEDINGS OF SCIENCE

# Updated Simulation of Airborne Neutrino Detectors for the PUEO Experiment

**William Luszczak**[*1,2] **for The PUEO Collaboration**

*E-mail:* wluszczak@icecube.wisc.edu

The upcoming Payload for Ultra-high Energy Observations (PUEO) experiment is planned for launch in the 2025/2026 season, and detailed simulation of the experiment is necessary for both the design of the instrument prior to launch, as well as data analysis post-flight. The new simulations package for PUEO builds upon the previously developed IceMC framework that was used by the ANITA experiment, and boasts a new model of the PUEO detector, including descriptions of the response of the antennas, amplification electronics, phased array trigger, and a more accurate parameterization of the Askaryan emission in ice that were not present in previous simulations. This improved simulation framework has since been used to provide a more accurate description of the projected capabilities of the PUEO experiment. Additionally, improvements in scalability and modularity of the codebase ensure that event sources, detector components, and even entirely new detectors can be easily added in the future.

[1] *Dept. of Astronomy, Ohio State University, Columbus, OH 43210, USA*
[2] *Dept. of Physics and Center for Cosmology and Astro-Particle Physics, Ohio State University, Columbus, OH 43210, USA*

[*] Presenter

The 38th International Cosmic Ray Conference (ICRC2023)
26 July – 3 August, 2023
Nagoya, Japan





PoS(ICRC2023)1154

## 1. Introduction

The Payload for Ultra-high Energy Observations (PUEO) experiment is planned for launch in late 2026, with the goal of studying the ultra-high energy neutrino flux [1]. Detector simulation is an important aspect of particle astrophysics research, as properly accounting for the detector response is key to obtaining a robust result. To this end, the PUEO collaboration has worked to develop an updated simulation package for use with the PUEO experiment. This simulation framework builds upon the previously existing IceMC simulation for the ANITA experiment [2], however unlike IceMC, the PUEO simulation framework is required to be more general, capable of handling not only additional sub-detectors like the planned low frequency instrument, but also coordinating signal simulation from a variety of potential RF sources (in-ice neutrinos, direct and reflected cosmic rays, and earth-skimming tau neutrinos). This contribution will focus on what has been introduced in the newer simulation framework of NiceMC and PueoSim that was not present in the older ANITA IceMC package.

## 2. Philosophy and Division of Responsibilities

We refactor and expand the IceMC package into an event generator responsible for Askaryan event simulation ("NiceMC") and a module describing the detector response ("PueoSim"). This division allows for the easy expansion of the simulation pipeline to include additional event generators describing other signal types (notably cosmic rays and earth-skimming tau neutrinos). This additionally allows for a straightforward implementation of the multiple sub-detectors comprising the PUEO payload, which contains both the main PUEO instrument as well as a planned low-frequency instrument comprised of independent antenna, trigger, and electronics.

A high-level map of the simulation process can be seen in figure 1. Users select one of the existing event generators and one or more detectors to simulate. Alternatively, NiceMC includes a virtual class for a generalized RF-neutrino detector, allowing users to implement their own detector descriptions if desired. The combination of event generator and detector(s) is then used to generate a signal pulse, which is then fed to the detector model. The detector model includes implementations of the antenna geometry and response, signal amplification chain, noise, and trigger. If multiple detectors are simulated, the response is evaluated in parallel, allowing for the examination of the same event in multiple detectors.

As the event generators for cosmic rays and tau neutrinos are currently a work-in-progress, the remainder of this contribution will discuss the simulation of in-ice Askaryan signals.

## 3. Askaryan Event Generation: NiceMC

The NiceMC event generator handles in-ice askaryan neutrino generation. Similar to the IceMC package, users provide the desired neutrino energy spectrum to NiceMC, and a flight path to PueoSim. The neutrino direction is chosen to be within detectable angles for the specified detector. If multiple detectors are simulated, only the first is used to determine the neutrino direction, though the response of the other detectors is still recorded.

In-ice neutrino interaction positions are determined by randomly picking positions along the simulated flight path. Positions are limited to occur near the horizon seen by the payload, and

neutrino directions are selected such that the detector lies close to the Cherenkov cone. Simulated neutrinos have directions uniformly distributed within $d\Theta$ of the angle that produces peak Askaryan emission, where $d\Theta$ is the angular width of the Askaryan pulse at the Cherenkov peak, and is characterized by the equations given in reference [3] for the electromagnetic component and reference [4] for the hadronic component. Note that due to this restriction of phase space, a direction weight is additionally calculated as the ratio of the solid angle spanned by the simulated region and the unit sphere, in order to account for the fact that events are only simulated from this restricted region, rather than isotropically over the full sky.

Once a neutrino energy, position, and direction have been selected, an Askaryan signal for that event is simulated. In place of detailed shower simulation, )which is prohibitively computationally intensive on large scales), the electric field 1 meter from the interaction location is parameterized according to reference [5]. This parameterization can easily be replaced with alternatives without affecting the rest of the simulation process, with an implementation of [6] being a current work in progress.

The propagation of the signal through ice and air has largely remained unchanged from the IceMC implementation, following the description in section 5 of reference [2].

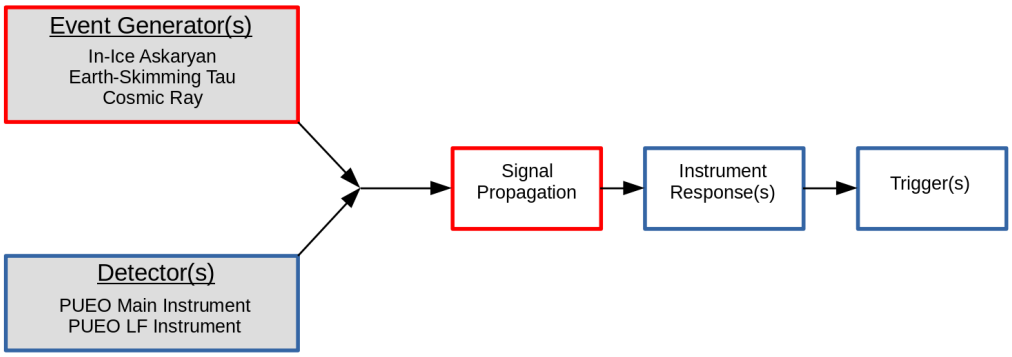


**Figure 1:** A high-level flowchart of the simulation procedure. Red boxes are implemented as part of NiceMC (the event generation package), while blue boxes are implemented as PueoSim (the detector simulation package). Note that the event generation requires some knowledge of the detector simulation due to the restricted phase space of simulations: events are only simulated if the detectors have a non-negligible chance to observe them.

## 4. PUEO Detector Simulation: PueoSim

### 4.1 Flightpath

As PUEO has not yet been launched, current options available for simulation are limited to previous ANITA flights. Flight path data is loaded from a data file, so this information can be easily updated following the first PUEO flight. Flight path information includes the longitude, latitude, altitude, yaw, pitch, and roll of the detector at any given time during the flight.

### 4.2 Payload Geometry

The PUEO main instrument is composed of 108 dual-polarization antennas: 96 regular antennas, and 12 nadir antennas tilted 30 degrees below the horizontal. Antenna positions and directions are loaded from included data files. With the exception of the nadir antennas, antennas are numbered according to azimuthal ($\phi$) sector and vertical antenna layer, following the pattern of (phi sector)+(antenna layer). The positive x-axis in payload coordinates is defined to be the direction of the face of antenna 0101, and the $+\phi$ direction is defined to be counter-clockwise around the payload as seen from above. Nadir antennas are then numbered separately with an "N" identifier.

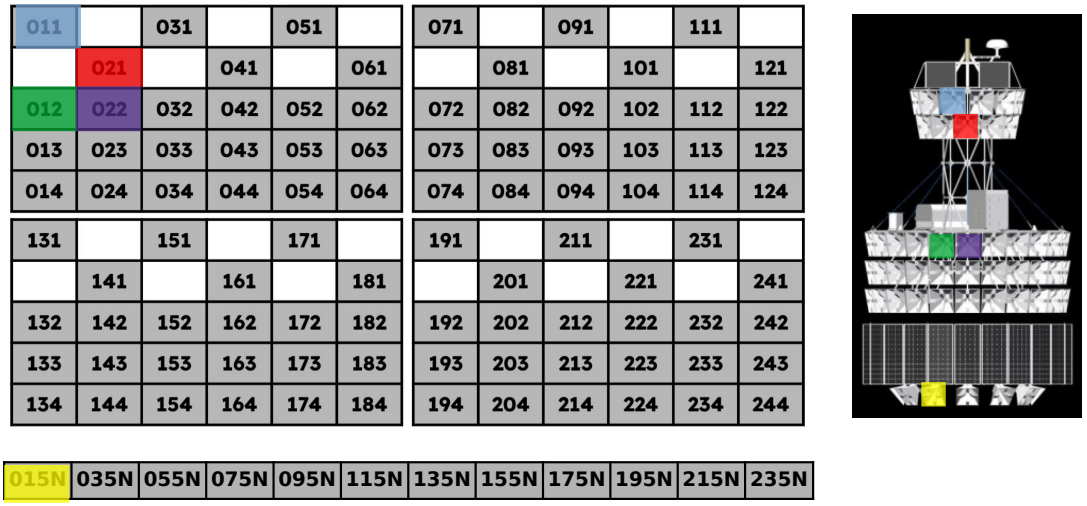


**Figure 2:** The PUEO antenna numbering system, with the positions of specific antennas highlighted on the payload diagram for reference. A "phi sector" encompasses a vertical group of 4 antennas (e.g. 011, 012, 013, and 014), and phi sector numbers increase in the counter-clockwise direction. For the purposes of this figure, the payload has been "wrapped" with the bottom two panels representing the far side of the payload. For example, phi sector 13 (antennas 131, 132, 133, and 134) is adjacent to phi sector 12 (antennas 121, 122, 123, and 124).

### 4.3 Antenna Response and RF Amplification Chain

After an event has been simulated and the signal propagated to the detector, the PUEO response is modeled via implementations of the generalized detector properties discussed above. The antenna and electronics chain responses are modeled via a series of transfer functions describing the gain and phase effects of each detector component. The antenna response is applied to the signal via a frequency-dependent antenna height factor. For the main PUEO instrument, this factor is obtained from laboratory measurements of the PUEO antenna prototypes, with included data files describing the boresight response, as well as the off-axis response in 10 degree increments. Unlike IceMC, which only characterized the antennas via their real-valued antenna gains, PueoSim incorporates the

antenna off-axis phase response via a complex-valued antenna height. Preliminary main instrument antenna responses as a function of angle are shown in Figure 3.

Following the application of the antenna response, the signal is amplified via a series of RF amplifiers. This RF amplification chain is modeled in its entirety by a single transfer function assembled from measurements of the amplification chain impulse response taken in the lab. Figure 5 shows the evolution of an example signal as the antenna and amplification chain responses are applied.

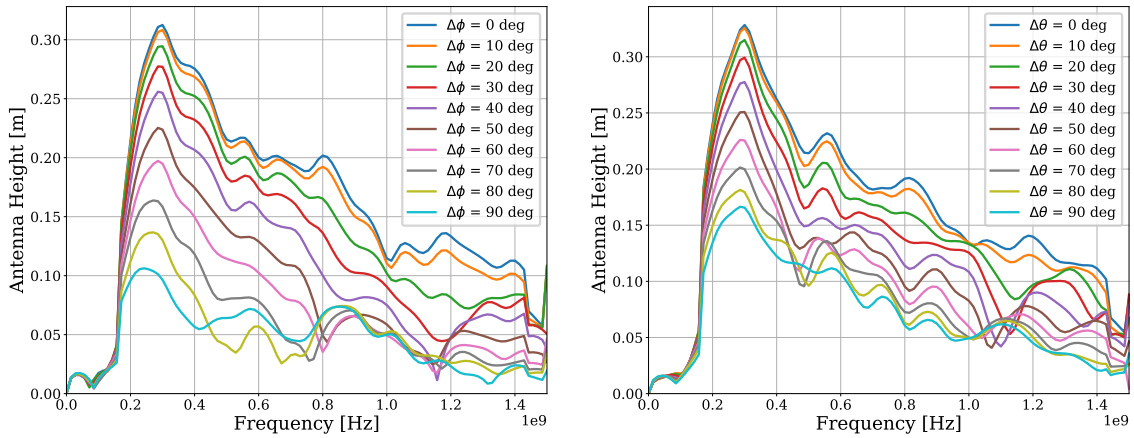


**Figure 3:** The PUEO main instrument antenna responses as a function of incident elevation angle ($\theta$), and azimuthal angle ($\phi$) in the local coordinate system of the antenna. The PUEO off axis response is modeled as a product of the boresight response with factors describing the variation of the response as a function of azimuth and elevation.

### 4.4 Noise

The PUEO simulation framework currently only includes thermal noise, though additional simulation of non-thermal noise will be added in the future. Thermal noise is generated according to a flat spectrum, and then bandwidth limited according to the response of the RF amplification chain. Additional system noise is added based on measurements of the amplification chain noise figure. An example noise waveform can be seen in Figure 4.

### 4.5 Trigger

PueoSim includes a new implementation of the planned phased-array trigger: signals on each antenna are delayed and coherently summed according to a hypothesis direction ("beams"), boosting the signal to noise ratio in the true direction of the incident radio pulse. If the power in the coherently summed signal exceeds a threshold value in any of the tested directions, the event passes the trigger. This process is done within a phi-sector of 8 neighboring antennas (L1), as well as with the neighboring phi sector as well (L2). The phased array trigger in PueoSim makes use of beams sized to be 20 degrees in azimuth and 4 degrees in elevation at the L1 level. Beams at the L2 level are half as large. These parameters are currently unoptimized, and are expected to change prior to the PUEO flight in 2025. However, as can be seen in figure 7, even simulations with an unoptimized

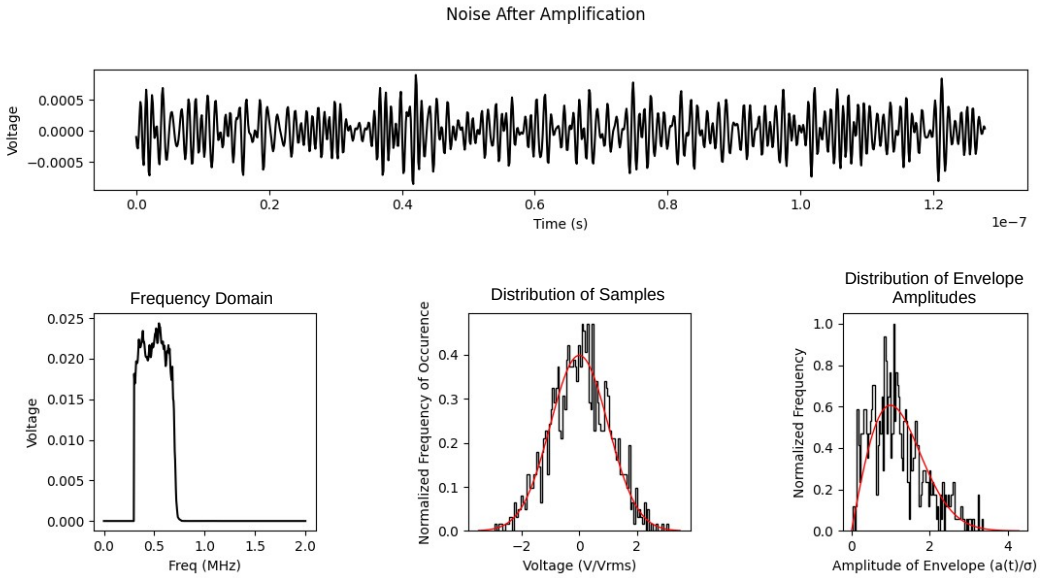


**Figure 4:** An example noise waveform in PUEO simulation (top), the noise spectrum in the frequency domain (bottom, left), the distribution of samples in the time domain with a gaussian with $\sigma = V_{rms}$ overlaid (bottom, middle), and the distribution of normalized envelope amplitudes with a Rayleigh distribution with Rayleigh parameter 1 overlaid (bottom, right).

phased array trigger still show significant improvement in comparison to previous experimental results, as well as previous estimates of PUEO sensitivity using scaled IceMC simulation.

## 5. Performance

The simulation framework described above has been used to update the sensitivity estimates of the PUEO main instrument, which had previously been obtained from scaled IceMC simulation. Updated sensitivies using NiceMC and PueoSim can be seen in Figure 7. An example simulated askaryan event can be seen in Figure 6, including both the main instrument and LF instrument waveforms. In comparison with previous estimates shown in (PUEO proposal), these updated estimates include detailed descriptions of the new PUEO antennas, amplification chain, and phased array trigger.

Future and in-progress uses for this simulation package include evaluating the effect of additional nadir antennas on event reconstruction, evaluating the impact of the low frequency instrument, and phased array trigger optimization. As PueoSim and NiceMC have been refactored to be significantly more modular than IceMC, studies involving substituting or adding detector components (or even entire subdetectors) can be easily performed. In particular, recent efforts towards using genetic algorithms to optimize RF antenna design [7] have begun using PueoSim to design antennas for use in PUEO-like airborne detectors. As this involves automatically switching out the antenna model with each iteration of the development loop, the modularity introduced in the PueoSim and NiceMC design is important in this context.

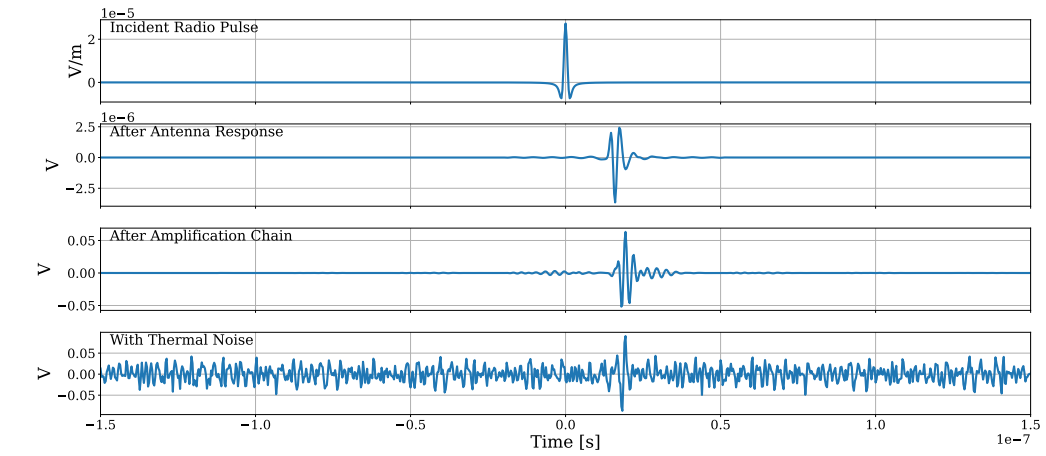


**Figure 5:** An example waveform on an individual antenna resulting from a simulated in-ice neutrino, at various stages of the simulation process. From top to bottom: After initial simulation and propagation to the payload, after the application of the off-axis antenna response factors, after amplification by the on-board electronics, and after the addition of thermal noise. The delay introduced between the top two panels is due to the travel time of the RF pulse between antennas: Antennas closer to the interaction see a signal earlier, while those farther away see a delayed signal.

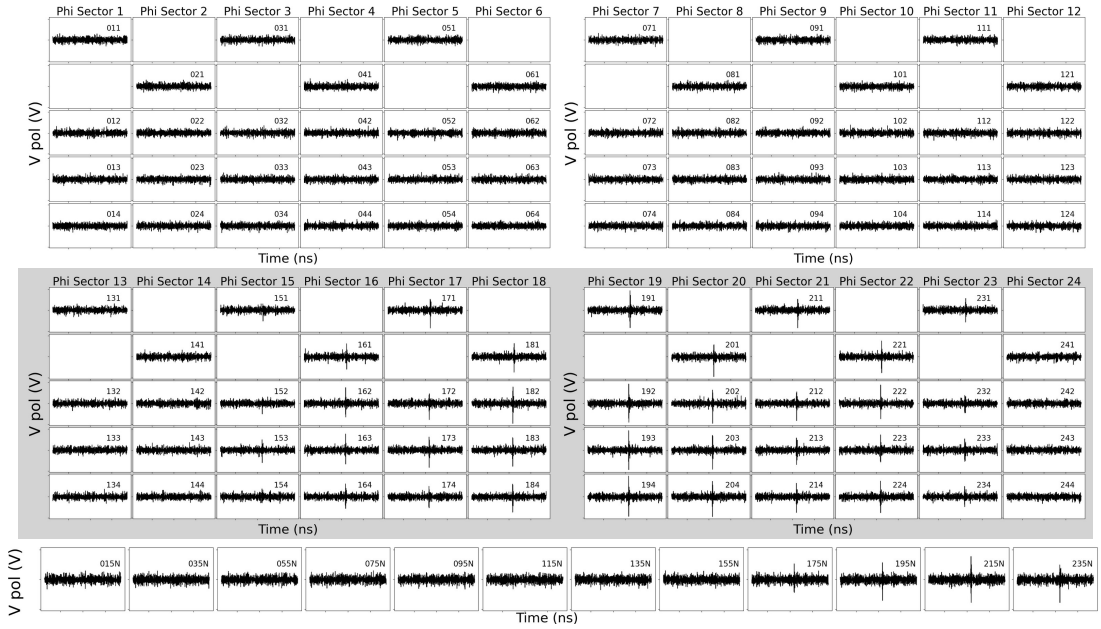


**Figure 6:** An event view of the V-pol waveforms for a simulated $10^{21}$ eV Askaryan neutrino that passed the PueoSim phased array trigger, originating from $\phi = 270°$ and $\theta = -8°$, corresponding to the brightest antennas being in phi sector 19. Main instrument antennas are shown in the top 4 panels, while nadir antennas (tilted down to 30 degrees) are shown at the bottom. Blank plots do not correspond to an antenna and are included only for the purposes of the graphical layout. The channels are numbered according to the scheme shown in figure 2

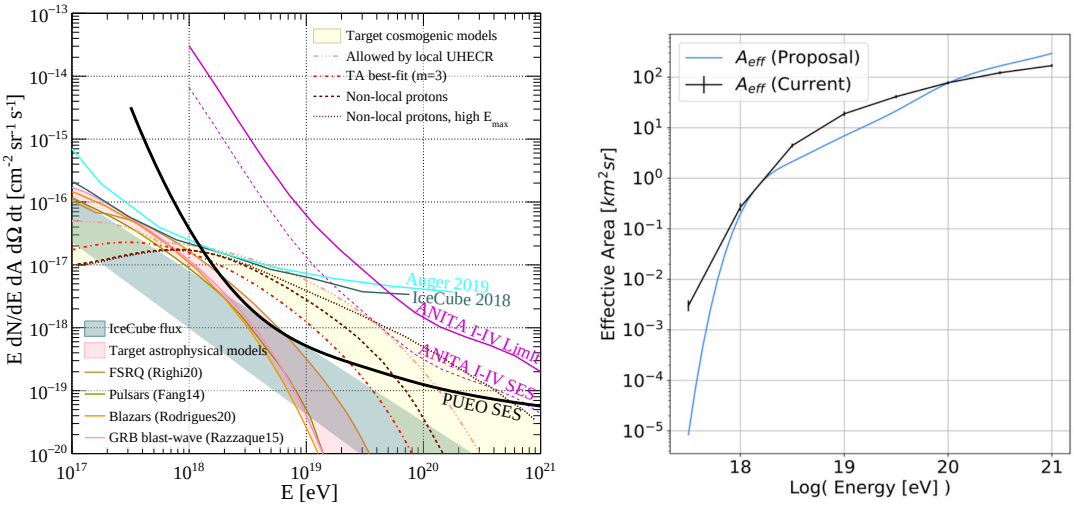


**Figure 7:** Left: The single event sensitivity of the PUEO experiment, computed using this simulation framework. In comparison to previous estimates shown in (original PUEO proposal), Right: A comparison of the PUEO effective area calculated using scaled ANITA simulation (blue), and the PueoSim/NiceMC framework discussed in this contribution (black).

## References

[1] **PUEO** Collaboration, Q. Abarr *et al.* *Journal of Instrumentation* **16** no. 08, (Aug, 2021) P08035.

[2] **ANITA** Collaboration, L. Cremonesi *et al.* *Journal of Instrumentation* **14** no. 08, (Aug, 2019) P08011–P08011.

[3] J. Alvarez-Muñiz and E. Zas *Physics Letters B* **411** no. 1-2, (Oct, 1997) 218–224.

[4] J. Alvarez-Muñiz and E. Zas *Physics Letters B* **434** no. 3-4, (Aug, 1998) 396–406.

[5] J. Alvarez-Muñ iz, R. A. Vázquez, and E. Zas *Physical Review D* **62** no. 6, (Aug, 2000) .

[6] J. Alvarez-Muñ iz, A. Romero-Wolf, and E. Zas *Physical Review D* **84** no. 10, (Nov, 2011) .

[7] J. Rolla, D. Arakaki, M. Clowdus, A. Connolly, R. Debolt, L. Deer, E. Fahimi, E. Ferstl, S. Gourapura, C. Harris, L. Letwin, A. Machtay, A. Patton, C. Pfendner, C. Sbrocco, T. Sinha, B. Sipe, K. Staats, J. Trevithick, and S. Wissel, "Evolving antennas for ultra-high energy neutrino detection," 2021.

## Full Author List: PUEO Collaboration

Q. Abarr[1], P. Allison[2], J. Alvarez-Muñiz[3], J. Ammerman Yebra[3], T. Anderson[4], A. Basharina-Freshville[5], J. J. Beatty[2], D. Z. Besson[6], R. Bose[7], D. Braun[7], P. Chen[8], Y. Chen[8], J. M. Clem[1], T. Coakley[2], A. Connolly[2], L. Cremonesi[9], A. Cummings[4], C. Deaconu[10], J. Flaherty[2], P. W. Gorham[11], C. Hornhuber[6], J. Hoffman[7], K. Hughes[4], A. Hynous[12], M. Jackson[2], A. Jung[11], Y. Ku[4], C.-Y. Kuo[8], G. Leone[10], C. Lin[1], P. Linton[2], T. C. Liu[13], W. Luszczak[2], S. Mackey[10], Z. Martin[10], K. McBride[2], C. Miki[11], M. Mishra[11], J. Nam[8], R. J. Nichol[5], A. Novikov[1], A. Nozdrina[6], E. Oberla[10], S. Prohira[6], R. Prechelt[11], H. Pumphrey[5], B. F. Rauch[7], R. Scrandis[10], D. Seckel[1], M. F. H. Seikh[6], J. Shiao[8,14], G. Simburger[7], G. S. Varner[11], A. G. Vieregg[10], S.-H. Wang[8], C. Welling[10], S. A. Wissel[4,15], C. Xie[5], R. Young[6], E. Zas[3], A. Zeolla[4]

[1]University of Delaware, [2]Ohio State University, [3]Universidade de Santiago de Compostela, [4]Pennsylvania State University, [5]University College London, [6]University of Kansas, [7]Washington University in St. Louis, [8]National Taiwan University, [9]Queen Mary University of London, [10]University of Chicago, [11]University of Hawaii, [12]NASA Wallops Flight Facility, [13]National Pingtung University, [14], [15]

PoS(ICRC2023)1154